

Seismic images and rock properties of the very shallow structure of Campi Flegrei caldera (southern Italy)

Dario Dello Iacono · Aldo Zollo · Maurizio Vassallo ·
Tiziana Vanorio · Sebastien Judenherc

Received: 25 January 2007 / Accepted: 9 May 2008 / Published online: 7 June 2008
© Springer-Verlag 2008

Abstract In September 2001, an extensive active-seismic investigation (Serapis experiment) was carried out in the Gulfs of Naples and Pozzuoli, with the aim of investigating and reconstructing the shallow crustal structure of the Campi Flegrei caldera, and possibly identifying its feeding system at depth. The present study provides a joint analysis of the very shallow seismic reflection data and tomographic images based on the Serapis dataset. This is achieved by reflection seismic sections obtained by the 3D data gathering and through refined P-velocity images of the shallowest layer of Pozzuoli Gulf ($z < 1,000$ m). From the refined V_p model, the overall picture of the velocity distribution confirms the presence of a complex arc-shaped anomaly that borders the bay offshore. The deeper part of the anomaly (beneath 700 m, with $V_p > 3,500$ m/s) correlates with units made up of agglomerate tuffs and interbedded lava, which form the southern edge of the caldera, which was probably formed following the two large ignimbritic eruptions that marked the evolutionary history of the area under study. The upper part of the anomaly that tends to split into two parallel arcs is correlated with dikes, volcanic mounds and hydrothermal alteration zones noted in previous shallow reflection

seismic analyses. The depth of the transition between the upper and lower parts of the anomaly is characterized by an abrupt V_p increase on the one-dimensional (1D) profiles extracted from the 3D tomographic model and by the presence of a strong reflector located at about 0.6/0.7 s Two Way Time (TWT) on Common Mid Point gathers. The move-out velocity analysis and stack of the P–P and P–S reflections at the layer bottom allowed to estimate relatively high V_p/V_s values (3.7 ± 0.9). This hypothesis has been tested by a theoretical rock physical modeling of the V_p/V_s ratio as a function of porosity suggesting that the shallow layer is likely formed by incoherent, water saturated, volcanic and marine sediments that filled Pozzuoli Bay during the post-caldera activity.

Keywords Campi Flegrei caldera · Shallow structure · Seismic reflection

Introduction

The volcanic field of Campi Flegrei is located in the central area of the Campanian plain, to the northwest of the Somma–Vesuvius complex. It covers a total area of around 200 km², which includes both on-land portions and the underwater vents in the area of Pozzuoli Gulf.

The Campanian plain is part of the eastern margin of the Tyrrhenian Sea, between 40° and 41° N, and it constitutes a large semi-graben from the superior Pliocene (5.3 My) that underwent pronounced subsidence during the Quaternary (more than 1,000 m/My, on average). The general structure of this semi-graben is easily recognizable at the edges of the plain, where the NE–SW- and SE–NW-oriented faults, that determined the gradual sinking of the carbonate rocks underneath thick layers of alluvial and pyroclastic Quaternary

Editorial responsibility: M. Ripepe.

D. Dello Iacono · A. Zollo (✉) · M. Vassallo · S. Judenherc
Dipartimento di Scienze Fisiche, Università di Napoli Federico II,
Napoli, Italy
e-mail: aldo.zollo@unina.it

T. Vanorio
Stanford Rock Physics Laboratory, Stanford University,
Stanford, CA, USA

S. Judenherc
Agecodagis, sarl,
Rieux Volvestre, France

deposits, can be seen (Ippolito et al. 1973; D'Argenio et al. 1973; Finetti and Morelli 1974; Bartole et al. 1984; Milia and Torrente 2003).

The volcanic activity of Campi Flegrei has been characterized by two main ignimbritic eruptions: that of the “Campanian Ignimbrite” (IC; 39 ka [De Vivo et al. 2001]) and that of the “Neapolitan Yellow Tuff” (TGN; 15 ka [Deino et al. 2004]). It is estimated that the first of these produced emissions of ca. 150/200 km³ of material, while the second produced emissions of ca. 40/50 km³ (Orsi et al. 1996, and references therein).

Although various aspects remain controversial, many studies have implicated one or both of these events as causal in the formation of the caldera (Rosi et al. 1983; Rosi and Sbrana 1987; Lirer et al. 1987; Barberi et al. 1991; Orsi and Scarpati 1989; Scarpati et al. 1993; Orsi et al. 1991, 1992, 1996; Wohletz et al. 1995), a wide sunken structure that forms part of Pozzuoli Gulf and the land area of Campi Flegrei (Agip 1987; Orsi et al. 1996; Zollo et al. 2003; Judenherc and Zollo 2004). After the formation of the caldera, the post-TGN volcanic activity was characterized by minor eruptions that formed the monogenic structures that have a circular distribution along the edge of the caldera, and the products of which have covered the collapsed structure.

The area is inhabited by around 400,000 people, who undergo an elevated risk from the still active magmatic system, which is well illustrated by the historic eruption of Monte Nuovo in 1538, by the recent ground upwelling episodes (1969–1972 and 1982–1984), by the fumarole activity, and by hot springs.

The definition of the structures that characterize the area and the knowledge of their relationships to the volcanic activity represent key elements for an understanding of the system and an evaluation of the associated volcanic hazard. For this reason, and in a first attempt to exploit the volcanic area as a geothermal source, the caldera structure has been investigated through gravimetric, magnetic, and local earthquake tomography investigations, as well as with drilled-rock sampling down to 3,000 m in depth (Rosi and Sbrana 1987; Agip 1987; Aster and Meyer 1988; Cassano and La Torre 1987; Florio et al. 1999; Capuano and Achauer 2003; Vanorio et al. 2005).

In September 2001, an extensive active seismic survey (Serapis Experiment) has been carried out in the Gulfs of Naples and Pozzuoli to reconstruct the structure of the Campi Flegrei caldera, to identify the presence and the form of potential superficial magma reservoirs, and to define the geometric relationships between the volcanic structures and the carbonate bedrock. These investigations have resulted in the identification of new, deep, structural features (Zollo et al. 2003; Judenherc and Zollo 2004):

- The identification in the Pozzuoli Gulf of a ring-like positive Vp anomaly, revealed between 750 and

2,000 m in depth (correlated with positive gravimetric anomalies [Capuano and Achauer 2003]);

- The identification of the off-shore extension of the Torre del Greco fault (a fault well described in the literature, and with a probable continuation towards the NE under the Somma–Vesuvius complex [Bruno et al. 1998]);
- The identification of a second fault of around 35 km in length that is parallel to the first to the west, and that starts from the southern coast of the Posillipo Hills and extends towards the SW, passing between the island of Ischia and Banco di Fuori (Zollo and Judenherc 2005).

All in all, the study has revealed the presence of the carbonate bedrock (average Vp velocity of 6,000 m/s) that is characterized by an irregular shape with a step-like structure that descends towards the NW, upon which the Campi Flegrei volcanic district, and more to the south that of the Somma–Vesuvius complex, have developed. The tomographic images have also allowed the identification and reconstruction of the geometry of the undersea part of the caldera.

The present study provide a detailed insight into the first kilometre of depth of the Pozzuoli Gulf, by determining the geometry and seismic properties of the volcano-clastic layer filling the shallowest part of the caldera.

The tomography data here presented are in support of the new analysis of seismic reflection and Vp/Vs relationships, but, in addition, they have contributed to the better definition of the 3D P-velocity model of the very shallow caldera structure, thus allowing for the correlation with the superficial volcanic structure of the bay noted by previous investigations.

Seismic reflection data analysis and modelling

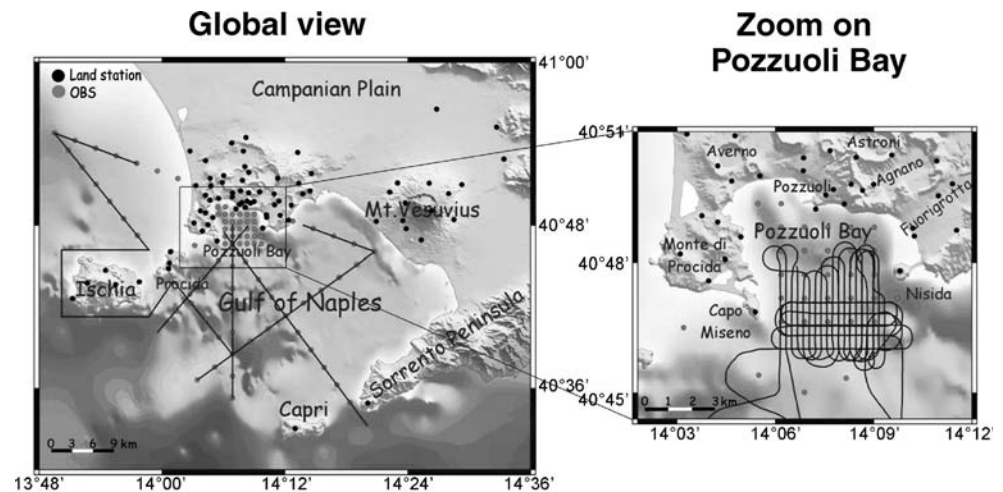
Data and methods

The dataset used for this study includes about 45,000 traces, and was extracted from the complete dataset collected for the Serapis project. The latter itself comprises more than 92,000 traces recorded with 70 OBS (sea-bottom receivers with 4.5 Hz 3-component sensors) and with 84 receivers on land (66 with 3-component sensors).

Shots were performed every 125 m on a grid with lines oriented N–S and E–W in Pozzuoli Bay (Fig. 1) (see also Judenherc and Zollo 2004, for more details).

To investigate the seismic properties of the very shallow layer filling the bay area, an analysis of P-to-P (PP) and P-to-S (PS) reflection arrivals was performed on the Serapis waveform dataset. Based on the acquisition layout of the experiment, a specific trace gathering scheme, that took

Fig. 1 Map of the area investigated during the Serapis experiment. The *square* is a zoom on Pozzuoli Gulf. The *black lines* trace the path of the vessel during the campaign. The *grey circles* display the positions of OBS, and the *black ones* the positions of land-stations deployed during the experiment



advantage of the potential of the 3D source–receiver geometry, was developed and applied to improve the detection and resolution of reflected/converted phases.

The vertical components of the recorded seismic waveforms were initially arranged in 3D Common Midpoint (CMP) gathers following the procedure described below. The Pozzuoli Bay area was subdivided into square cells and the midpoint position between the corresponding source and receiver was calculated for each trace considered, taking as maximum offset a distance of 2,000 m. All of the records with the midpoint falling in a given cell have therefore been grouped into the same CMP, independent of the source–receiver azimuth. This is equivalent to assuming a near vertical variation in the velocity distribution in a cone, pointing down in the Earth at the cell centre, and having a diameter of 2,000 m at the surface (Fig. 2a).

After several trials, a cell size of 500×500 m was chosen based on the criteria of having a sufficiently high number of traces in each CMP gather (>30) and a dense coverage of the explored area, while maximum offset was chosen based on the duplex criteria that the lateral variations of the velocity had to be negligible with respect to those vertical, and along the sections the morphology of the interface had to be more or less planar and horizontal. Figure 2b shows the geometry of the cells considered and the number of records for each cell (Fig. 2c).

Given the distribution of the sources and receivers in the Serapis experiment, the cells with a higher number of records are those in the central part of the Bay, between Capo Miseno and the peninsula of Nisida, where gathers contain more than 120 recordings.

The following processing steps were then applied to the CMP gathers:

- Band-pass filtering using a Butterworth filter with cut-off frequencies of 5 Hz and 15 Hz;
- Automatic gain control using a 1-s window;
- Trace normalization (Fig. 3a);

- Normal moveout (NMO) correction, using velocities determined by the CVS method (Fig. 3b);
- Refined picking of the main PP reflections on vertical records and single phase static correction using picked arrival times. This procedure is applied to remove unmodelled 3D effects arising from an imperfect knowledge of the propagation medium and local complex reflector morphology (Fig. 3c);
- Graphic display of the seismic sections and analysis of the lateral coherency of reflection events by visual comparisons of different gathers along the EW and NS profiles (Fig. 3d).

Moreover, to support the new reflection seismic analyses, and to correlate the results with superficial geological structures, we produced a refined 3D V_p model (Fig. 4), referred to the first kilometer depth of Pozzuoli Bay, obtained using the same inversion method and data described in Judenherc and Zollo (2004). In addition, we performed a manual refined re-picking of the first arrivals followed trace by trace on all of the record sections. This procedure, allowed us to improve the quality of the model at shallow depths as evidenced by an overall reduction in the residuals distribution with distance with respect to results obtained by Zollo et al. (2003) and Judenherc and Zollo (2004), although the long wavelength features of the two models remain very similar.

Analysis of the horizontal component: NMO correction for PS and estimates of the best V_p/V_s value

The velocity analysis is a tool widely used as a first order correction of the propagation effects also in complex geological contexts. Indeed, even when the background velocity is heterogeneous and the interface is irregular, the variation induced in the propagation times is generally smaller than the propagation times of the reflected/converted waves. In this case, the perturbations in the

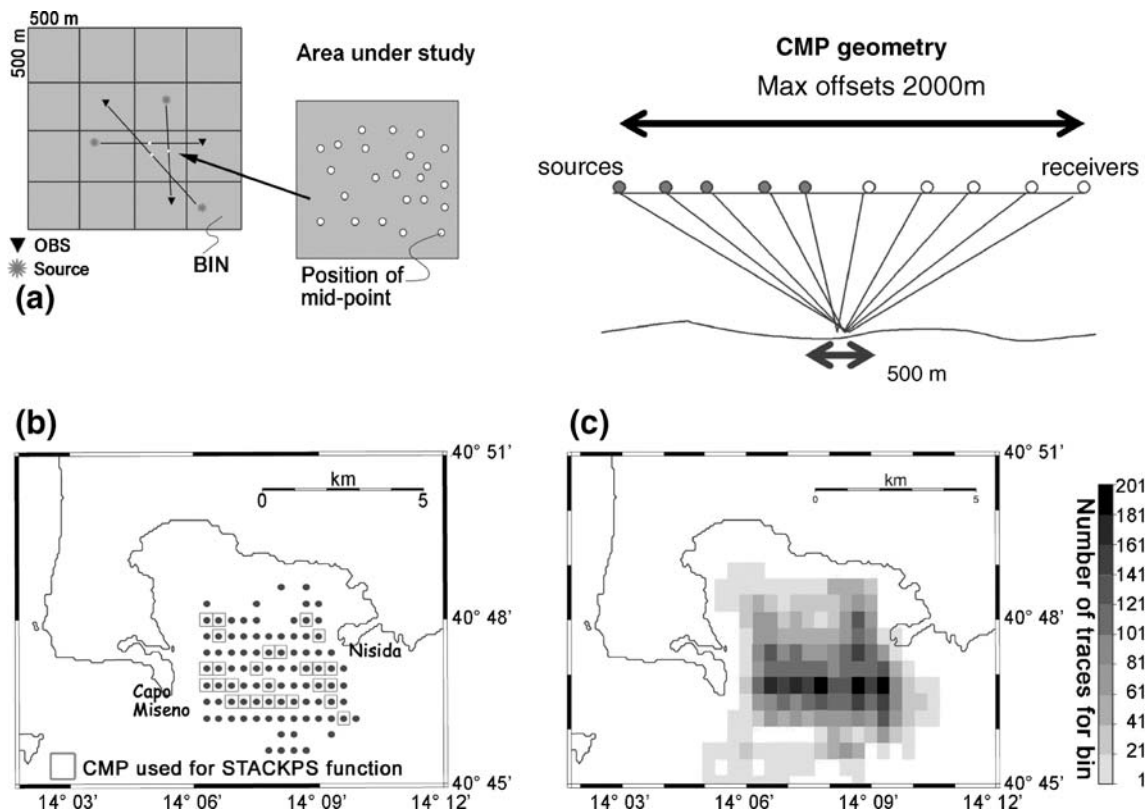


Fig. 2 **a** Geometry used to organize traces in 3D CMP gathers. The Pozzuoli Bay area was subdivided into square cells (500×500 m) and the midpoint position between the corresponding source and receiver was calculated for each trace considered, taking as maximum offset a distance of 2,000 m. All of the records with the midpoint falling in a

given cell have therefore been grouped into the same CMP, independent of the source–receiver azimuth. **b** Map with position of bin (*the point shows the centre of the cell*). The CMPs within the *square* were used for calculation of STACKPS function. **c** Density map showing the number of traces in each cell

arrival times do not prejudice the determination of the alignment of the phases in the NMO sections.

A posteriori, the data can demonstrate the validity of the correction carried out. Indeed, in the case of extreme heterogeneity of the velocity and/or a highly irregular reflecting surface, we would expect that the corrected NMO sections are dominated by diffractions, rather than by aligned phases; but when it is possible to recognize a coherent alignment of the phase on many adjacent sections we can assert that the reflector is nearly horizontal and the medium above it can be represented, as a first approximation, by an uniform wave velocity model.

Taking in mind these assumptions we performed a velocity analysis both on vertical and radial component.

The two-way times of the PP reflected arrival have been picked from the vertical component sections and corrected for a moveout velocity of 1,600 m/s. We have chosen CMPs 1031, 1073, 1111, 703, 705, 745, 827, 868, 907, 908, 949, 950 which show relatively high signal-to-noise ratios for the PP phase and a good lateral coherency. A total of 1,108 readings of the PP arrival times were performed for an average value of 0.64 s two-way traveltimes with a standard deviation of 0.06 s.

Assuming the average two-way time of the PP phase as the zero-offset time for the identified reflector, and using the average P-velocity profile as inferred from seismic tomography in the Pozzuoli Bay area, one can obtain an interface depth of $600 \text{ m} \pm 120 \text{ m}$. The depth uncertainty is increased by propagating the errors on time picks (0.06 s) and on P-velocity (200 m/s) through the formula $h = (T_0 V_p) / 2$.

The V_p/V_s ratio was estimated for each CMP by a moveout analysis of the PS phases on the radial component, i.e. the horizontal component oriented in the source-to-receiver direction (Jurkevics 1988). Given the average interface depth and layer P-velocity, the theoretical travel time of a PS phase can be calculated for a given value of the V_p/V_s ratio. Then a narrow window (0.3 s) is selected on the radial component CMP section, beginning at the estimated arrival time of the PS phase. For each V_p/V_s value limited in a defined range (1.5, 5.5), we evaluated the following stack function:

$$STACKPS(V_p/V_s) = \sum_{t=T_{Theo}^{PS}}^{T_1^{PS}} \left(\sum_{i=1}^{N_{sis}} A_i(t) \right)^2$$

where T_{Theo}^{PS} is the theoretical PS travel time for a given V_p/V_s value, and $T_1^{PS} = T_{Theo}^{PS} + 0.3 \text{ s}$; $A_i(t)$ is the amplitude at

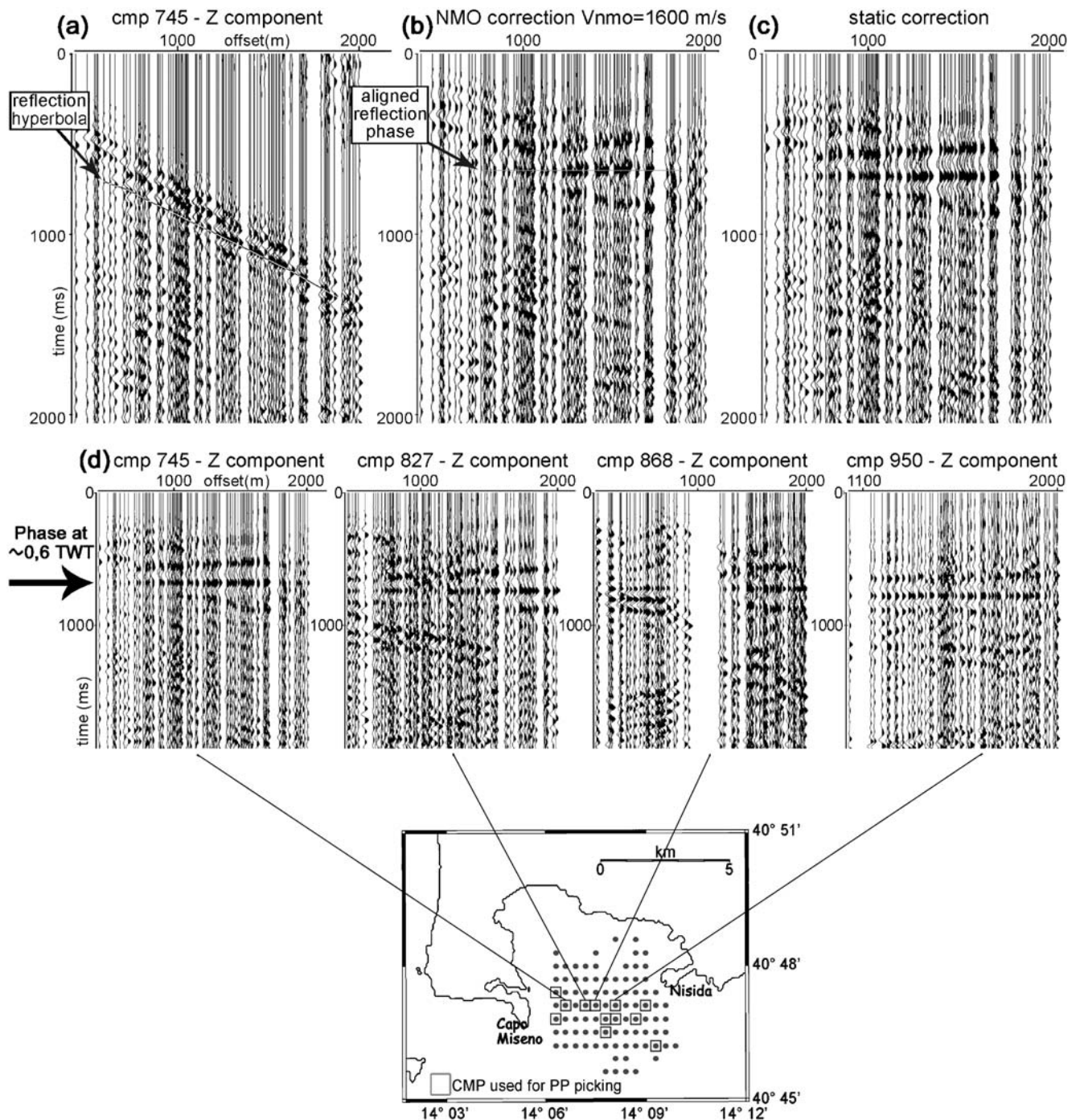


Fig. 3 **a** Example of CMP gather section (745) after filtering, AGC and normalization. Note the reflection hyperbola with apex at about 0.6/0.7 s TWT emphasized by black/white line. **b** NMO correction of the previous section, with $V_{nmo}=1,600$ m/s. Note aligned reflection phase at about 0.6/0.7 s TWT indicated by the arrow and grey line. **c**

Static phase correction at 0.7 s TWT. **d** Example of presence and coherency of superficial reflected phase at 0.6/0.7 s on adjacent CMPg sections (vertical component) highlighted by the arrow. In the below map, the position of CMPg is shown. The CMPs within the square were used for calculation of PP picking

time t for the i th seismogram, and N_{sis} is the number of seismograms contained in a given CMP section.

The function STACKPS vs V_p/V_s has been computed for the CMPs indicated in Fig. 2b using a step of 0.01 in the V_p/V_s quantity. We selected 27 CMP sections for which a relatively high number of traces was available (>60) and

which had a good offset coverage (at least 750 m to 1,950 m). Several examples of STACKPS functions are given in Fig. 5a, where the functions have been normalized to their maximum values. For the selected CMPs, the shape of the STACKPS function, centered at V_p/V_s values ranging between 3.0 and 4.0, generally showed a single,

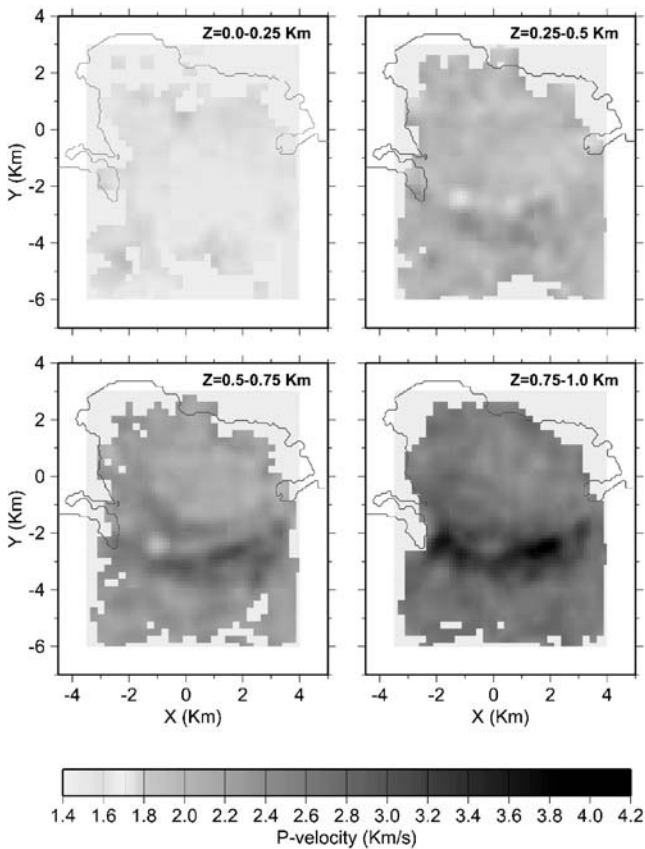
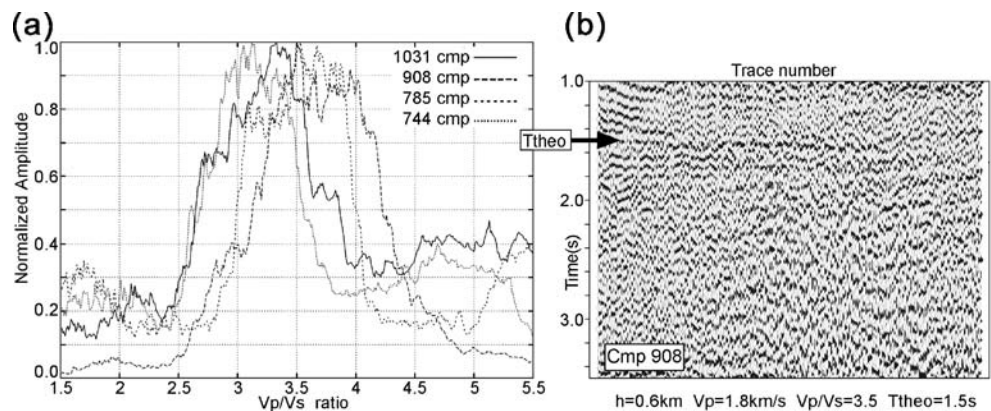


Fig. 4 Plane views of the velocity model. *Light grey* indicate low velocities, and *dark grey* indicate high velocities. For each layer, the top and bottom depths of the layer are indicated. Land topography is indicated with a *solid line*. *Peripheral light grey* indicates not resolved area for insufficient or absent ray coverage. Note double-arc shape P-velocity anomaly in the section 0.5–0.75 km, stretching between Nisida and Capo Miseno

broad peak, whose amplitude is related to the inhomogeneity of the superficial layer above the interface, to the morphology of the reflector, and to the noise of the data that prevents a perfect alignment of the P–S reflected seismic phase after the NMO correction.

An estimate of the Vp/Vs ratio at each CMP is obtained by the value corresponding to the maximum of the STACKPS function. Figure 5b shows an example of the

Fig. 5 **a** Examples of STACKPS functions normalized to their maximum values. The function generally shows a single, broad peak centered at Vp/Vs values ranging between 3.0 and 4.0. **b** Example of the PS moveout corrected radial section at CMP 908 using the value of Vp/Vs which maximizes the relative STACKPS function



PS moveout corrected radial section at CMP 908 using the values of Vp/Vs which maximize the relative STACKPS function. This example shows good agreement between the aligned PS phase and the theoretical travel-time estimate.

To obtain the average value of Vp/Vs and related uncertainty by using the estimated values, we performed a statistical analysis of the variable $A = \log\left(\frac{V_p}{V_s}\right)$. We used log quantities because the log-normal probability density is adequate to represent probability distributions for quantities expressed by the ratio of random variables, as Vp/Vs that by definition are constrained to be positive (Tarantola 2005).

We defined the uncertainty δA_i on each estimate A_i , as the half-width of the function STACKPS(A) at a level equal to half of the maximum amplitude. The weighted average \bar{A} of A_i values is calculated by using the weighting factors w_i defined as $w_i = 1/(\delta A_i)^2$. The standard error associated to the quantity \bar{A} is computed through the formula:

$$\sigma_A = \sqrt{\frac{\sum_i w_i (A_i - \bar{A})^2}{\sum_i w_i} + \sum_i \frac{(\delta A_i)^2}{N}}$$

which accounts for the statistical error depending on the spatial variability of Vp/Vs ratio and for the measurement error which instead depends on the shape of the function STACKPS related to the signal-to-noise level on waveforms and misalignments on NMO corrected sections. The values of \bar{A} and σ_A computed by using the procedure above, provided an estimate of the Vp/Vs ratio of $V_p / V_s = 3.7 \pm 0.9$.

Discussion

The joint analysis of seismic reflection sections and tomographic images has provided new information about the shallow structure of the Campi Flegrei caldera in correspondence with its southern border and inner region.

In the following we discuss on data evidences and interpret our results by using previous outcomes obtained

from gravimetric, seismic activity, and drilled-rock sampling analyses, conducted in Pozzuoli Gulf and on land, on the basis that the velocity distribution and impedance contrasts can be associated with the elastic characteristics, and thus ultimately to the lithology of the medium under investigation.

The most important result has been the identification and characterization of the volcano-clastic layer filling the shallowest part of the caldera. The tomographic analysis, performed in support of the new investigations of seismic reflection and of V_p/V_s relationships, was able also to better define the complex vertical development of the arc-shaped high P-velocity anomaly, stretching from Nisida to Capo Miseno (Judenherc and Zollo 2004), allowing for the correlation with the superficial volcanic structure of the bay.

Very high resolution seismic tomography and shallow volcanic structures

Tomographic images reveal a correlation between P-velocity anomaly at 0.5–0.75 km in depth (Fig. 4) that tends to split into two parallel arcs, and the position of dikes, volcanic structures and the off-shore fumaroles detected in the Gulf of Pozzuoli (Fig. 6) (De Bonitatibus et al. 1970; Pescatore

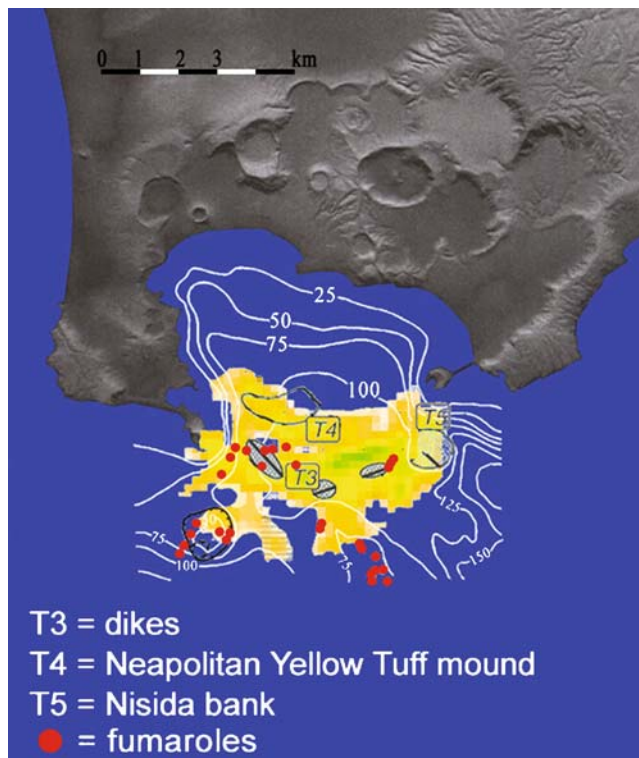


Fig. 6 Correlation between the position of the double-arc V_p anomaly and the positions of fumaroles, dikes, the TGN mound and Nisida Bank in the Bay of Pozzuoli (structures identified in De Bonitatibus et al. 1970; Pescatore et al. 1984; Milia 1998; Milia and Torrente 2003). White lines display the bathymetry of the bottom of the bay. For volcanic structure, we used the same symbols and the same acronyms like in Milia and Torrente (2003)

et al. 1984; Milia 1998; Milia and Torrente 2003). The presence of these structures suggests the existence of a highly fractured area, through which the magma and gases may have been able to rise towards the surface.

In a similar way, the post-TGN eruptive activity on land has been concentrated along the northern edge of the caldera. Analogous models simulating caldera collapses (Acocella et al. 2000, 2004) have shown how the formation of caldera structures is accompanied by the development of faults in concentric rings, normal and inverse, with large angles, and that these fractured areas can represent preferential routes for the rise of magma towards the surface.

The analysis of the 1D velocity profiles extracted from the 3D tomographic model shows a steep change in the P wave velocity at about 600 m in depth (Fig. 7). Above that depth, V_p values range from 1,500 to 2,000 m/s and indicate the presence of a thick, low velocity sediment formation filling the shallower part of the caldera. In contrast, from 600 m down to 900 m in depth, the P wave velocity increases sharply from 2,000 to 2,600 m/s. This velocity discontinuity is also confirmed by seismic reflection data.

Evidence for a thick, low V_p , high V_p/V_s , water saturated layer

The analysis of the vertical component CMP gathers located on the southern border of the Bay of Pozzuoli has

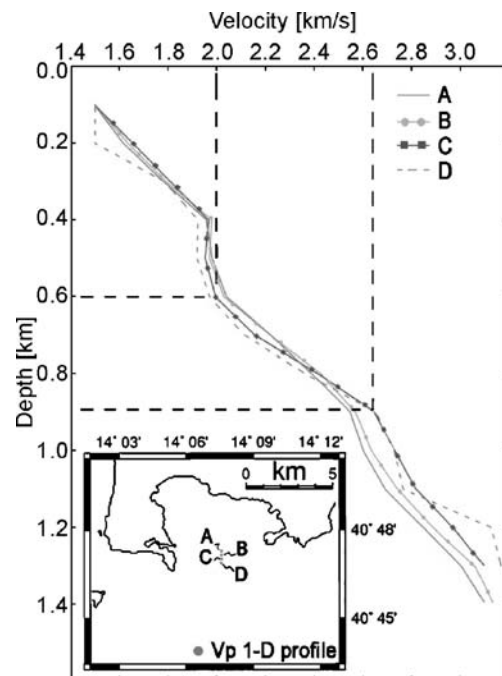


Fig. 7 One-dimensional V_p profiles extracted from NS vertical tomographic sections. Note the abrupt increase in V_p between 600 and 900 m in depth. The map shows position of profiles

shown the presence of a strong amplitude reflection event at 0.6–0.7 s TWT, which aligns for a NMO correction of 1,600–1,800 m/s, and corresponds to an approximate reflector depth of 600–800 m. By close inspection of the CMP gathers, we discovered that this seismic discontinuity is revealed with continuity and lateral coherency in the whole external area of Pozzuoli Bay (Fig. 3d).

The joint modeling of PP and PS reflections on vertical and radial component CMP gathers allowed the constraining of the average Vp-to-Vs ratio in the shallow sediment to 3.7 ± 0.9 . This value is much higher with respect to those found in the literature (Aster and Meyer 1988; Vanorio et al. 2005; Chiarabba and Moretti 2006; Battaglia et al. 2008), where previous tomography studies have provided ratios around 2 for the first kilometer in depth.

The value obtained, together with the estimated P-wave velocities, provide shear-wave velocities of 450–515 m/s. The robustness of this result is confirmed by the clear alignment of the PS arrivals at the theoretical arrival times on moveout radial sections obtained by using $V_p = 1,600$ –1,800 m/s and Vp/Vs values that maximize the stack function defined in the previous paragraph (Fig. 5b).

It is worth noting that the high Vp/Vs ratio represents an average estimate of the whole shallow layer, and thus such a value could be strongly influenced by the saturation conditions of the rocks in the first hundreds of meters.

Concerning the origin of the strong velocity contrast generating the high amplitude reflection event at about 0.6–0.7 s TWT, we note that the stratigraphic profiles of in-land boreholes in the Mofete area, located on the northern border of the caldera, show the evidence of a thick trachitic and latitic lava layer at about 750 m under tuff and tuffites post-caldera. The velocity contrast, as indicated by laboratory measures of density and Vp on rock samples taken from the wells (Vanorio 2003), can generate a reflective wave of great amplitude.

Although it remains speculation, in terms of the known difficulties in volcanic areas for correlations over large distances, the location of the CMP gathers analysed is in the southern sector of the caldera rim. So it appeared reasonable to hypothesize a lithological succession similar to that of the North-West sector, with the difference in the sedimentation environment that would have characterised the deposition of the products lying on the lava layer.

While the activity gradually became sub-aerial in the northern part of the caldera, in the southern sector, the present gulf of Pozzuoli, the conditions of marine sedimentation can have persisted since the caldera collapse except for the Würmian phase (about 18 kyr bp), when the sea level reached –120 m and all the area had emerged (Pescatore et al. 1984). The thick, low Vp, shallow layer under study, formed by volcanic and marine sediments that filled up the bay during the post-caldera phases of activity

of Campi Flegrei, could therefore include incoherent pyroclastic rocks and chaotic tuffs, highly water saturated because of marine sedimentation.

Theoretical rock physical modeling of the Vp/Vs ratio vs porosity

A layer with such physical characteristics could have important repercussions on the modelling and general understanding of the processes that form the basis of the slow up/down-welling episodes in the caldera.

In order to test our hypothesis, we modeled the variation of the Vp/Vs ratio as a function of porosity in unconsolidated sediments, withstanding pressure conditions appropriate to describe the layer lying above 600 m. The elastic properties of rocks are known to be controlled by the properties of the solid frame, such as composition and grain contact stiffness, and pore fluid and porosity. High Vp/Vs ratios have been shown to characterize shallow water-flow sediments in water depths between 400 m and 2,000 m below the seabed (Huffman and Castagna 2001).

At such depths of burial, these materials are poorly consolidated (i.e. low grain contact stiffness) and undergo low effective stresses. That makes them exist near a transition between rocks and sediments characterized by a

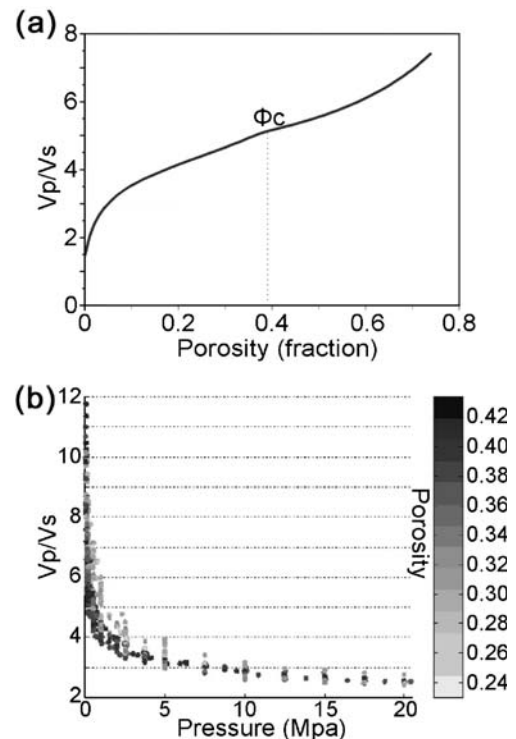


Fig. 8 **a** Variation in the Vp/Vs ratio as a function of porosity in unconsolidated, water-saturated sediments. The critical porosity is 0.38 and the number of contacts per grain is 8.5. **b** Vp/Vs ratio data for water-saturated glass-bead samples plotted against the effective pressure. Data are in grey scale as a function of porosity (from Zimmer 2003)

critical porosity Φ_c (Nur et al. 1991, 1995). This Φ_c critical porosity separates the mechanical behavior of rocks into two distinct domains: for porosities lower than Φ_c , the mineral grains are load-bearing, whereas at porosities greater than Φ_c , sediments fall apart and behave as a mineral-pore suspension. We theoretically reproduced the effects of poorly consolidated sediments lying at 500 m on the elastic properties, via modeling as proposed by Dvorkin et al. 1999.

The lower Hashin–Shtrikman bound is the most appropriate model as we were simulating the elastic properties of unconsolidated sediments and, therefore, looking for the softest rock arrangement. Figure 8a shows the variation of the V_p/V_s ratio as a function of porosity for an unconsolidated quartz-sand having a critical porosity of 38%. Figure 8a shows that the V_p/V_s ratio increases with increasing porosity, as in fluid-bearing sediments, shear wave velocity approaches zero while the compressional-wave velocity does not fall below the velocity of a suspension of sand in water.

Zimmer (2003) showed a similar trend in the V_p/V_s ratio (Fig. 8b) for a set of reconstituted, unconsolidated sand and glass-bead samples under low pressure conditions. The modeling results and the experimental measurements reported for unconsolidated sediments (Zimmer 2003) suggest that the large changes predicted in the V_p/V_s ratio at low effective pressures (Fig. 8a, b) are consistent with the hypothesis of poorly consolidated, fully water saturated sediments lying above 600 m in depth.

Nevertheless, it should be emphasized that the results in Fig. 8 have to be considered purely indicative of the magnitude of the V_p/V_s trends. The lack of the input parameters for site-relevant poorly consolidated rocks as well as the V_p/V_s calculated as a average over a layer thickness of 600 m prevents us from considering the modeling of Fig. 8a for quantitative purposes.

Conclusions

The present study has provided detailed information about the elastic properties of the sediments in the first kilometer of depth of the Pozzuoli bay and the correlations with volcanic structure known by previous investigations, by using a new reflection seismic analysis and a refined tomographic model.

The overall picture of the velocity distribution shows the presence of a complex arc-shaped anomaly that borders the bay offshore. The deeper part of the anomaly (beneath 700 m, with $V_p > 3,500$ m/s) correlates with units made up of agglomerate tuff and interlayered lava, which form the southern edge of the caldera, which was itself probably formed following the two large ignimbritic eruptions that

marked the evolutionary history of the area under study. The upper part of the anomaly is correlated with dikes, volcanic mounds and hydrothermal alteration zones noted in previous shallow reflection seismic analyses.

The depth of the transition between the upper and lower parts of the anomaly is characterized by an abrupt V_p increase on the one-dimensional (1D) profiles extracted from the 3D tomographic model and by the presence of a strong reflector located at about 0.6/0.7 s Two Way Time (TWT) on Common Mid Point gathers. The moveout velocity analysis and stack of the P–P and P–S reflections at the layer bottom allowed to estimate relatively high V_p/V_s values (3.7 ± 0.9).

This hypothesis has been tested by a theoretical rock physical modeling of the V_p/V_s ratio as a function of porosity suggesting that the shallow layer is likely formed by incoherent, water saturated, volcanic and marine sediments that filled Pozzuoli Bay during the post-caldera activity.

The presence of a superficial layer with such characteristics could have important implications on the modelling and general understanding of the processes that form the basis of the bradyseism of the zone.

References

- Acocella V, Cifelli F, Funicello R (2000) Analogue models of collapse calderas and resurgent domes. *J Volcanol Geotherm Res* 104:81–96
- Acocella V, Funicello R, Marotta E, Orsi G, De Vita S (2004) The role of extensional structures on experimental calderas and resurgence. *J Volcanol Geotherm Res* 129:199–217
- Agip (1987) *Geologia e Geofisica del Sistema Geotermico dei Campi Flegrei*. Servizi Centrali per l' Esplorazione, SERG-MMESG, San Donato, 19 pp
- Aster RC, Meyer RP (1988) Three-dimensional velocity structure and hypocentral distribution in the Campi Flegrei caldera, Italy. *Tectonophysics* 149:195–218
- Barberi F, Neri G, Valenza M, Villari L (1991) 1987–1990 unrest at Vulcano. *Acta Vulcanologica* 1:95–106
- Bartole R, Savelli D, Tramontana M, Wezel F (1984) Structural and sedimentary features in the Tyrrhenian margin of Campania, Southern Italy. *Marine Geology* 55:163–180
- Battaglia J, Zollo A, Virieux J, Dello Iacono D (2008) Merging active and passive data sets in travelttime tomography: the case study of Campi Flegrei caldera (Southern Italy). *Geoph Prosp*. In press
- De Vivo B, Rolandi G, Gans PB, Calvert A, Bohrsen WA, Spera FJ, Belkin HE (2001) New constraints on the pyroclastic eruptive history of the Campanian volcanic Plain (Italy). *Mineral Petrol* 73:47–65
- Bruno PPG, Cippitelli G, Rapolla A (1998) Seismic study of the Mesozoic carbonate basement around Mt. Somma-Vesuvius, Italy. *J Volcanol Geotherm Res* 84:311–322
- Capuano P, Achauer U (2003) Gravity field modeling in the Vesuvius and Campanian area. In: Zollo A et al (ed) *TomoVes Seismic Project: looking inside Mt. Vesuvius*. Cuen, Napoli
- Cassano E, La Torre P (1987) Geophysics, in Santacroce R (ed), *Somma-Vesuvius*. CNR Quaderni della Ricerca Scientifica 114 (8):175–192

- Chiarabba C, Moretti M (2006) An insight into the unrest phenomena at the Campi Flegrei caldera from Vp and Vp/Vs tomography. *Terra Nova* 18:373–379
- D'Argenio B, Pescatore T, Scandone P (1973) Schema geologico dell'Appennino meridionale. *Atti dell' Accademia Nazionale dei Lincei* 183:49–72
- De Bonitatibus A, Latmiral G, Mirabile L, Palumbo A, Sarpi E, Scalera A (1970) Rilievi sismici per riflessione: strutturali, ecografici (fumarole) e batimetrici del Golfo di Pozzuoli. *Boll Soc Nat* 79:97–115
- Deino AL, Orsi G, Piochi M, de Vita S (2004) The age of the Neapolitan Yellow Tuff caldera-forming eruption (Campi Flegrei caldera—Italy) assessed by $^{40}\text{Ar}/^{39}\text{Ar}$ dating method. *J Volcanol Geotherm Res* 133:157–170
- Dvorkin J, Prasad M, Sakai A, Lavoie D (1999) Elasticity of marine sediments: rock physics modeling. *Geophys Res Lett* 26 (12):1781–1784
- Finetti I, Morelli C (1974) Esplorazione sismica a riflessione dei Golfi di Napoli e Pozzuoli. *Boll Geof Teor Appl* 16(62/63):175–222
- Florio G, Fedi M, Cella F, Rapolla A (1999) The Campanian Plain and Campi Flegrei: structural setting from potential field data. *J Volcanol Geotherm Res* 91:361–379
- Huffman A, Castagna J (2001) The petrophysical basis for shallow water flow prediction using multicomponent seismic data. *The Leading Edge* 20(9):1030–1052
- Ippolito F, Ortolani F, Russo M (1973) Struttura marginale tirrenica dell' Appennino Campano: reinterpretazione di dati di antiche ricerche di idrocarburi. *Mem Soc Geol Ital* 12:227–250
- Lirer L, Luongo G, Scandone R (1987) On the volcanological evolution of Campi Flegrei. *EOS, Trans Am Geophys Union* 68:226–234
- Judenherc S, Zollo A (2004) The Bay of Naples (Southern Italy): constraints on the volcanic structures inferred from a dense seismic survey. *J Geophys Res* 109:B10312
- Jurkevics A (1988) Polarization analysis of three-component array data. *Bull Seismol Soc Am* 78(5):1725–1743
- Milia A (1998) Stratigrafia, strutture deformative e considerazioni sull' origine delle unità deposizionale oloceniche del Golfo di Pozzuoli (Napoli). *Boll Soc Geol Ital* 117:777–787
- Milia A, Torrente M (2003) Late-Quaternary volcanism and transtensional tectonics in the Bay of Naples, Campanian continental margin, Italy. *Mineralogy and Petrology* 79:49–65
- Nur A, Marion D, Yin H (1991) Wave velocities in sediments. In: Hovem J, Richardson MD, Stoll RD (eds) *Shear waves in marine sediments*. Kluwer, Norwell, pp 131–140
- Nur A, Mavko G, Dvorkin J, Galmundi D (1995) Critical porosity: the key to relating physical properties to porosity in rocks. *Proc 65th Ann Int Meeting. Soc Expl Geophys* 878
- Orsi G, Scarpati C (1989) Stratigrafia e dinamica eruttiva del Tufo Giallo Napoletano. *CNR-GNV Boll* 2:917–930
- Orsi G, Civetta L, Aprile A, D'Antonio M, de Vita S, Gallo G, Piochi M (1991) The Neapolitan Yellow Tuff: eruptive dynamics, emplacement mechanism and magma evolution of a phreatoplinian-to-plinian eruption. In: *Large Ignimbrite Eruptions of the Phlegraean Fields Caldera: The Neapolitan Yellow Tuff and The Campanian Ignimbrite*. G. Orsi and M. Rosi, Editors, I.A.V.C.E.I. Commission on Explosive Volcanism, Workshop on Explosive Volcanism, Naples, Sept. 1–8, Guideb., pp. 76–115.
- Orsi G, D'Antonio M, De Vita S, Gallo G (1992) The Neapolitan Yellow Tuff, a large-magnitude trachytic phreatoplinian eruption: eruptive dynamics, magma withdrawal and caldera collapse. *J Volcanol Geotherm Res* 53(1–4):275–287
- Orsi G, De Vita S, Di Vito M (1996) The restless, resurgent Campi Flegrei nested caldera (Italy): constraints on its evolution and configuration. *J Volcanol Geotherm Res* 74:179–214
- Pescatore T, Diplomato G, Senatore MR, Tramutoli M, Mirabile L (1984) Contributi allo studio del Golfo di Pozzuoli: aspetti stratigrafici e strutturali. *Mem Soc Geol Ital* 27:133–149
- Rosi M, Sbrana A (1987) Phlegraean Fields. *CNR Quaderni della Ricerca Scientifica* 114(9):175
- Rosi M, Sbrana A, Principe C (1983) The Phlegraean Fields: structural evolution, volcanic history and eruptive mechanisms. *J Volcanol Geotherm Res* 17:273–288
- Scarpati C, Cole P, Perrotta A (1993) The Neapolitan Yellow Tuff: a large volume multiphase eruption from Campi Flegrei, Southern Italy. *Bull Volcanol* 55:343–356
- Tarantola A (2005) Inverse problem theory and methods for model parameter estimation. *SIAM*, Philadelphia, 342 pp
- Vanorio T (2003) Physical properties of volcanic rocks from Campania plain. In: Capuano P, Gasparini P, Zollo A, Virieux J, Casale R, Yeroyanni M (eds) *The internal structure of Mt. Vesuvius. A seismic tomography investigation*. Liguori, Naples, pp 553–580
- Vanorio T, Virieux J, Capuano P, Russo G (2005) Three-dimensional seismic tomography from P wave and S wave microearthquake travel times and rock physics characterization of the Campi Flegrei Caldera. *J Volcanol Geotherm Res* 110:B03201
- Wohletz K, Orsi G, De Vita S (1995) Eruptive mechanism of the Neapolitan Yellow Tuff interpreted from stratigraphic, chemical and granulometric data. *J Volcanol Geotherm Res* 67:263–290
- Zimmer M (2003) Controls on the seismic velocities of unconsolidated sands: measurements of pressure, porosity and compaction effects. Ph.D. thesis, Stanford University, Stanford, CA
- Zollo A, Judenherc S (2005) Reply to comment by Rapolla A on The Bay of Naples (southern Italy): constraints on the volcanic structures inferred from a dense seismic survey. *J Geophys Res* 110:B06308
- Zollo A, Judenherc S, Auger E, D'Auria L, Virieux J, Capuano P, Chiarabba C, De Franco R, Ma kris J, Michelini A, and Musacchio G (2003) Evidence for the buried rim of Campi Flegrei caldera from 3-d active seismic imaging. *Geophys Res Lett* 30(19); DOI 10.1029/2003GL018173